International Journal of Thermofluid Science and Technology (2023)
Volume 10, Issue 3, Paper No. 100303
https://doi.org/10.36963/IJTST.2023100303

Research Article

Blood flow transport with electrokinetic flow technique through a narrow semicircle shape within the vertical 2D asymmetrical model

Suwimon Saneewong Na Ayuttaya

Department of Mechanical Engineering, Academic Division, Chulachomklao Royal Military Academy, Nakhon Nayok, Thailand

ATICLE INFO

Received: 21 June 2023;
Received in revised form:
5 July 2023;
Accepted: 09 July 2023;
Published online:
15 July 2023

Keywords:
Blood flow transport,
Narrow semicircle shape,
Electrokinetic flow technique,
2D asymmetrical model.

ABSTRACT

Within the vertical 2-Dimensional (2D) asymmetrical model, the blood flow transport through a narrow semicircle shape is the numerical study based on the concept of the electrokinetic flow technique. In this study, the blood flow transport has been compared to the electric field, the flow pattern, the pressure field, the vorticity, the temperature field, and the concentration field with and without the electrokinetic flow. The electrical voltage and time are varied from 0 – 20 kV and 0 – 1 s, respectively. The result has shown that the blood flow transport is moved upward within the vertical 2D asymmetrical model and the electric field has not appeared in the case of without the electrokinetic flow. With the electrokinetic flow, the flow pattern, the pressure field, the vorticity field, the temperature field, and the concentration field are not the same pattern as the electric field but they are induced by the electric field. Furthermore, at the center of a narrow semicircle shape, the electric value, the velocity, and the pressure are increased with the electrical voltage increasing but the vorticity and concentration are decreased with the electrical voltage increasing. Finally, the experimental result is compared with the numerical result, it can be seen that simulation results had good agreement with experiment results.

1. Introduction

The electrokinetic flow technique is defined as the migration of bulk ionic fluid due to the interaction between an applied electric field tangentially along a charged surface and the excess net charge density in the electric double layer of such a charged surface. Therefore, electrokinetic flow in porous media is referred to as the motion of bulk ionic liquid flowing through a sample as a result of the interplay of an applied electric field and the excess charge density in the electric layer of the charged structure [1 - 4]. Furthermore, the electrokinetic flow technique can be used as an active technique to improve mixing in various devices for other applications such as electrokinetic pumping [5 - 7], electrospray droplet [8 - 9], electrostatic precipitator [10 - 11], heat transfer enhancement by applying electric field [12 - 15]. An electrokinetic pump in which the porous dielectric medium of conventional electrokinetic pumps is replaced by a patterned microstructure. The channel structure provides the electric field necessary for electroosmotic flow [16]. A new technology for implanted electrical

*Corresponding e-mail: joysuwimon@gmail.com (Suwimon Saneewong Na Ayuttaya)

Nomenclature

b	ion mobility, m^2/Vs	V	electrical voltage, V
C_p	specific heat capacity, J/kgK	r, z	axisymmetric
c	concentration, mol/m^3	*Greek symbols*	
D	diffusion coefficient, cm^2/s	ε	dielectric permittivity, F/m
	electric flux density, C/m^2	ε_T	relative permittivity, F/m
E	electric field, V/m	η	kinematics viscosity, m^2/s
f_E	electric force, C/m^2s	μ	viscosity, kg/ms
g	gravity, m/s^2	ρ	density, kg/m^3
J	current density, A/m^2	σ	relative conductivity, s/m
k	thermal conductivity, W/mK	μ	viscosity, kg/ms
n	unit normal vector	*Subscripts*	
P	pressure, N/m^2	i	initial
q	space charge density, C/m^3	0	tip of electrode
T	temperature, K	*Superscript*	
t	time, s	T	matrix transpose
v	vertical velocity, m/s		

heart pumps in the treatment of heart failure. Heart failure is an important and growing public health problem. This technique is used for biomechanics in order to increase the cardiovascular system that pumps blood to the heart [17 - 18].

Biomechanical treatment or biomechanical physical therapy can be summarized as the application of biomechanics to the diagnosis and treatment of patients [19 - 20]. It is involving more than one discipline or field of study. Treatment and therapy require a multidisciplinary approach involving medical, mechanical, and electrical sciences. Electrokinetic pumping systems are one of the multidisciplinary sciences and some researchers are studied disease treatment and therapy such as Midura et al. [21] studied the healing of fibular osteotomies enhancement by pulsed electromagnetic field treatments. The result had shown that the apparent modulus of each callus was assessed via a cantilever bend test and indicated a 2-fold increase in callus stiffness in the pulsed electromagnetic field treatment over sham-treated fibulae. The pulsed electromagnetic field treatment fibulae exhibited an apparent modulus at the end of 5 weeks that was 80% that of unoperated fibulae. Lebovka et al. [22] studied the effects of thermal and moderate electric field treatment on the damage of sugarbeet tissue. The results showed that the electrically stimulated damage of a sugarbeet tissue occurred even at a rather small electric field strength if the treatment time was large. The energy consumption caused by moderate electric field treatment was mainly related to temperature elevation inside the tissue and noticeably decreased with increasing electric field strength. Moderate electric field treatment was experimentally investigated in the aqueous media revealing the dependence of damage efficiency on sample orientation with respect to the external electric field. Miranda et al. [23] studied the electric field distribution in the brain during the application of such tumor-treating fields. A realistic head model was constructed and placed in transducer arrays. The results had shown that the regions of local field enhancement occurred near interfaces between tissues with different conductivities wherever the electric field was perpendicular to those interfaces. These increases were strongest near the ventricles but were also present outside the tumor's necrotic core and in some parts of the gray matter-white matter interface. The electric field could be reduced cancer cell proliferation in vitro. The electric field distribution was highly non-uniform and depended on tissue geometry and dielectric properties.

Electro-osmotic is the flow of liquid that is in contact with a charged solid surface when an electric field is applied. The pump uses electro-osmotic flow to provide a high pressure hydraulic system in order to biomechanical treatment [24 - 27].

The multidisciplinary approaches are investigated such as Venkateswarlu and Bhaskar [24] analyzed the MHD flow of an incompressible and electrically conducting Casson fluid in a micro-channel. It could be that the Casson parameter accelerated the skin-friction coefficient while it provided resistance to the rate of heat transfer near the channel walls. Bhatti et al. [25] studied the electro-osmotic flow of non-Newtonian fluid. The mathematical modeling was based on the Poisson–Boltzmann equation, Debye length approximation, and ionic Nernst Planck equation. The present effects were beneficial in designing and manufacturing microfluidics device to determine the transport mechanism. Dadsetani et al. [26] studied the efficiency of electronic equipment. The results shown that the tangential hybrid method could decrease the peak temperature and peak Von Mises stress, up to 40% and 34% in comparison to the microchannel and high-conductivity inserts method. Zeeshan et al. [27] investigated the electrokinetic microperistaltic pumps for biomechanical devices. For mathematical modelling, the solid particles were distributed the flow in a channel with complex waves. The defined flow problem was modelled and analyzed analytically for the transport of a solid–liquid suspension.

Coronary artery disease is a condition that affects your heart. It is happening when coronary arteries struggle to supply the heart with enough blood, oxygen and nutrients. Cholesterol deposits or plaques in the heart arteries and inflammation are usually the cause of coronary artery disease. In the previous study, the electrical heart pumps in the treatment of heart failure have a little studied by researchers. Due to biomechnaical model, electrokinetic flow technique has a very complex interaction between the electrostatic field, flow field, concentraton field and temperature field. In this research area, the concept of biomechanical treatment by the electrokinetic flow technique is systematically studied. This research is an assumption on the artery attached to the skin or thin layer of skin and behind the multidisciplinary research approach involving medical and electrokinetic flow techniques can be used as the cornerstone of the technology development. of cardiovascular disease therapy.

2. Description of the biomechanics therapy by the electrokinetic flow

Coronary artery disease is caused by plaque buildup in the wall of the arteries that supply blood to the coronary arteries. Fig. 1 shows the diagram of blood flow transferred from downstream to upstream within the coronary artery. The geometry of normal and blocked arteries is shown in Fig. 1 (a) and (b), respectively. Plaque is made up of cholesterol deposits and plaque buildup causes the inside of the arteries to narrow over time. The electrostrictive hydrodynamics (*EHD*) generator is the biomechanics therapy by the electrokinetic flow. It is the increased flow mechanism and the pressure of the blood flow is increased. Fig. 2 shows the diagram of biomechanics therapy by the electrokinetic flow. The electric discharge is created from the *EHD* generator through the plaque deposits zone within the coronary arteries so coronary artery disease can be therapy. It is the new concept of biomechanical treatment by the electrokinetic flow technique.

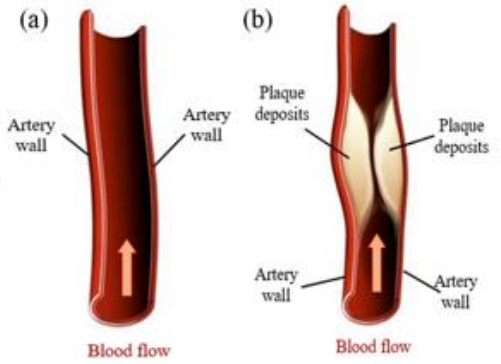

Fig. 1 The diagram of coronary arteries (a) normal artery (b) blocked artery by plaque deposits

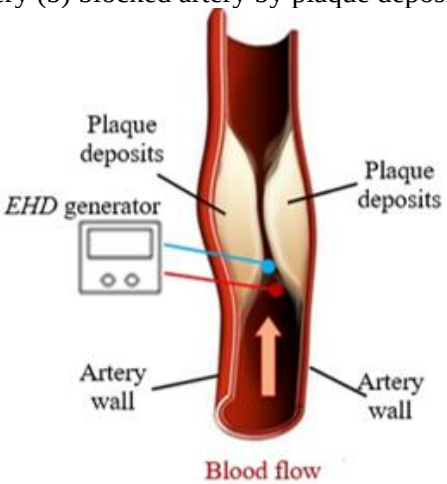

Fig. 2 The diagram of biomechanics therapy by electrokinetic flow.

Fig. 3 shows the boundary conditions of coronary arteries and the Finite Element Method (FEM) using a collocation method used for solving problems of algebraic equations. FEM is a numerical method for solving partial differential equations in two or three space variables. It is a numerically solving differential equations arising in engineering and mathematical modeling. To solve a problem, the FEM subdivides a large system into smaller and this is achieved by a particular space discretization in the space dimensions [28 - 29]. The boundary condition is the flow and concentration field model as shown in Fig, 3 (a). For the flow and the concentration field model, the inlet velocity and the inlet concentration boundary conditions (v_i, P_i, c_i) are assumed to be uniform. The outlet boundary condition of the blood flow is considered with no viscous stress ($\eta(\nabla\vec{v}+(\nabla\vec{v})^T\cdot n=0$, $\vec{P}=\vec{P}_0$), and the convective flux of the concentration ($n\cdot(-D\nabla\vec{c})=0$). In the case of the blocked artery by plaque deposits within the coronary artery, Fig. 3 (b) shows the boundary conditions of the flow and concentration field model. It represents the plaque deposits that are stuck at the artery wall and it is set out of the boundary condition. The artery walls are applied at no slip ($\vec{v}=0$). This is the standard and default boundary condition for a stationary solid wall. The biomechanics therapy by electrokinetic flow is shown in Fig. 3 (c). The two boundary conditions are composed of the electrostatic model and the flow and concentration field model. For the electrostatic model, the boundary conditions of all outer sides are considered as zero charge symmetry ($n\cdot D=0$). The electrode and ground are considered electrical voltage ($V=V_0$) and ground ($V=0$) boundary conditions, respectively. In this research area, the concept of biomechanics therapy by the electrokinetic flow is systematically studied. This research is an assumption on the artery attached to the thin layer of skin and behind the multidisciplinary research can be used as prediction guidance for the special design of the biomechanical of heart disease therapy with the electrokinetic flow model.

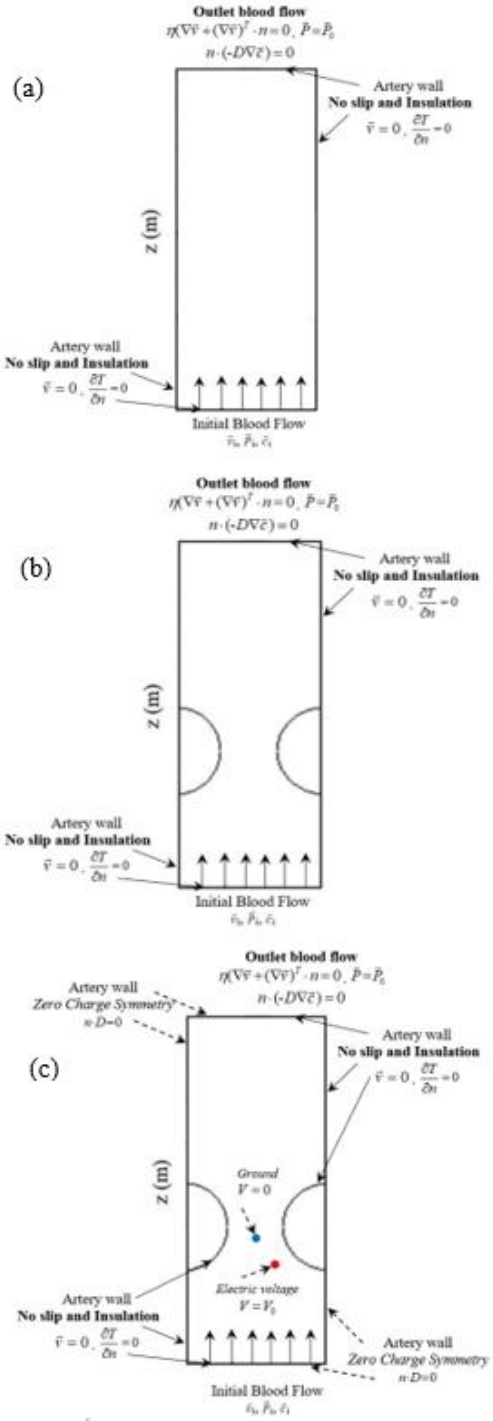

Fig. 3 The boundary conditions of coronary arteries (a) normal artery (b) blocked artery by plaque deposits (c) biomechanics therapy of blocked artery by electrokinetic flow

3. Methodology

For the prediction of biomechanics therapy by the electrokinetic flow technique, the physical model, the model approach, the problem definition, the boundary condition, and the calculation procedure systematically investigated the blood flow transport from the electrokinetic flow effect.

3.1 Equation

Mathematical modeling based on the concept of an electrokinetic flow technique has been developed for the prediction of the blood flow transport through a narrow semicircle shape within the vertical 2-Dimensional (2D) asymmetrical model.

For the electrostatic model, this study is developed to predict the electric field distribution computed from Maxwell's equations listed below:

$$\nabla \cdot \varepsilon \vec{E} = q \tag{1}$$

$$\vec{E} = -\nabla V \tag{2}$$

$$\nabla \cdot J + \frac{\partial q}{\partial t} = 0 \tag{3}$$

$$J = q\vec{v} + (\vec{v} \cdot \nabla)(\varepsilon \vec{E}) - b\nabla q \tag{4}$$

where E is electric field intensity, q is the space charge density in the fluid, ε is dielectric permittivity, V is electrical voltage, J is current density, b is ion mobility and v is vertical blood flow velocity.

The governing equation for computing the electric force (f_E) performing on blood flow can be expressed by

$$\vec{f}_E = q\vec{E} - \frac{1}{2}\vec{E}^2\nabla\varepsilon + \frac{1}{2}\nabla\left[\vec{E}^2\left[\frac{\partial\varepsilon}{\partial\rho}\right]_T \rho\right] \tag{5}$$

where ρ is the density of fluid and space charge density (q) is described by Griffiths [30]. It is a concept in which excess electric charge is treated as a continuum of charge distributed over a region of space.

From the right-hand side of Eq. (5), three terms are the electrophoretic, the dielectrophoretic, and the electrostrictive forces, respectively. In the first term, the electrophoretic force results from the net uncharged within the fluid or ions injected from the electrodes. Electric field distribution is emitted from the electrode and induced to the ground. For the second and the third terms of Eq. (5), the dielectrophoretic force is a consequence of inhomogeneity in the permittivity of the dielectric fluid and the electrostrictive force is caused by non-homogeneous electric field strength and the variation in dielectric constant with temperature and density. For the modeling analysis assumption, the dielectric properties are constant, and homogeneity and magnetic field effect are neglected. Therefore, dielectrophoretic and electrostrictive forces are negligible.

For the flow and the concentration field model, the incompressible fluid and the fluid physical properties are assumed to be constant and the effect of buoyancy and emission or absorption of radiant energy is negligible. The continuity equation is considered in Eq. (6) and Navier–Stokes equations which are coupled with the electrophoretic force equation are considered in Eq. (7).

$$\frac{\partial\rho}{\partial t} + \nabla \cdot (\rho\vec{v}) = 0 \tag{6}$$

and

$$\rho\left[\frac{\partial\vec{v}}{\partial t} + (\vec{v} \cdot \nabla)\vec{v}\right] + \rho g = -\nabla\vec{P} + \mu\nabla^2\vec{v} + \vec{f}_E \tag{7}$$

where P is pressure and μ is viscosity.

For the temperature field model, the effect of the phase change can be neglected and the thermal properties of the fluid are considered to be constant. For the species concentration equation for a transient state, the temperature distribution is calculated by energy equation as shown in Eq. (8) and the diffusion coefficient is constant this equation can be written as Eq. (9):

$$\rho C_p\left[\frac{\partial T}{\partial t} + \vec{v}\nabla T\right] = k\left(\nabla^2 T\right) \tag{8}$$

and

$$\rho\left[\frac{\partial\vec{c}}{\partial t} + (\vec{v} \cdot \nabla\vec{c})\right] = \nabla \cdot (-D\nabla\vec{c}) \tag{9}$$

where C_p is the specific heat capacity and k is thermal conductivity c is concentration and D is the diffusion coefficient.

3.2 Configuration

The coronary artery is assumed to be a vertical 2D asymmetrical model. This axially symmetric surface is comprised of mainly three parts, the first part is the electrostatic model, the

second part is the flow and concentration field model and the third part are the temperature model. Fig. 4 shows the physical model geometry of the 2D axisymmetric cylindrical tube with a radius (r) is 3 mm (0.003 m) and a long (z) is 14 mm (0.014 m). The plaque deposits are assumed to be a semicircle shape and the radius of plaque deposits is 1 mm (0.001 m). It represents the plaque deposits (semicircle shape) that are stuck at the artery wall and it is set out of the boundary condition. In order to study the blood flow transportation within the vertical 2D asymmetrical model with the electrokinetic flow, the electrode, and ground are a very small circle and the diameter is 0.005 mm. The position of the single electrode and the single ground is always fixed at (- 0.001, 0) and (- 0.002, 0.001), respectively. The configuration under investigation in the present study consists of an axially symmetric model where initial blood flow (v_i, P_i) was entered by Montienthong et al. [31] and it flows from bottom to top. In this study, electrical voltage (V_0) and time (t) are varied in a range of 0 – 20 kV and 0 – 1 s, respectively. The blood is a non-Newtonian fluid and its viscosity changes depending on how much stress is placed on it. The initial normal blood concentration (c_i) is 24 mol/m^3 (24 mmol/L) [32] and the uniform initial temperature (T_i) of blood is 310 K [33]. The classical and thermophysical properties of the blood within the vertical 2D asymmetrical model are shown in Table 1 [33].

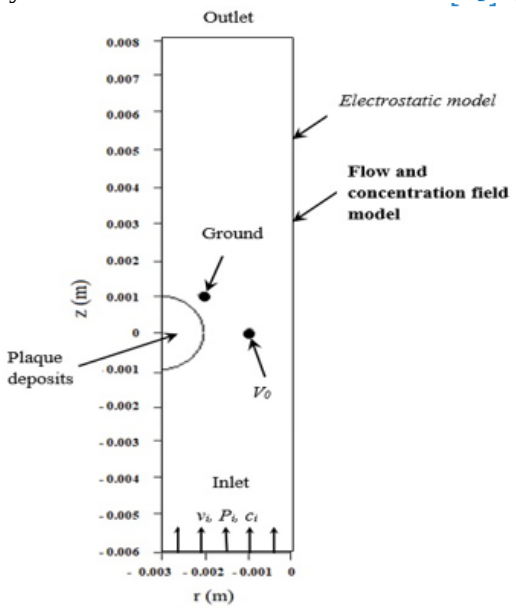

Fig. 4 The physical model geometry of the vertical 2D asymmetrical model

Table 1 Classical and thermal properties of blood within the vertical 2D asymmetrical model from Wessapan et al. [33]

Properties	Blood
Thermal conductivity (k (W/mK))	0.497
Temperature ($T(t_i)$ (K))	310
Density (ρ (kg/m^3))	1,030
Specific heat capacity (C_p (J/kgK))	3,600
Relative permittivity (ε_r (F/m))	43.00
Relative conductivity (σ (S/m))	1.69

3.3 Boundary condition

A boundary condition of the vertical 2D asymmetrical model with the electrokinetic flow technique has been developed for the prediction of the blood flow transport through a narrow semicircle shape, as shown in Fig. 5. Half of the diagram in Fig. 2 is the research problem in this study.

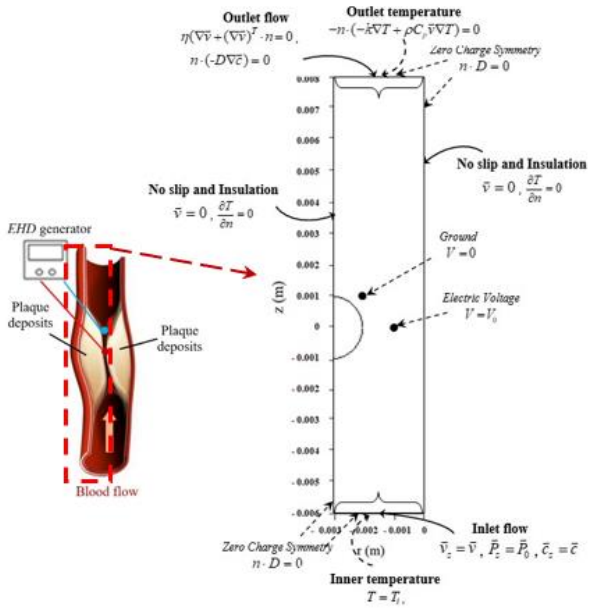

Fig. 5 Boundary conditions for analysis

For the electrostatic field boundary condition, all of the outer side boundary conditions are considered as zero charge symmetry are considered in Eq. (10) and

$$n \cdot D = 0 \qquad (10)$$

Electrode and ground are considered as electrical voltage (Eq. (11)) and ground (Eq. (12)) boundary conditions, respectively.

$$V = V_0 \quad \text{at electrode position} \quad (11)$$

$$V = 0 \quad \text{at ground position} \quad (12)$$

where n is the unit normal vector and D is electric flux density.

For the flow and the concentration field boundary condition, the blood flow transport flows from downstream to upstream through a narrow semicircle shape. The inlet velocity (Eq. (13) and (14)) and the inlet concentration (Eq. 15) boundary conditions are assumed to be uniform. It is defined as:

$$\vec{v}_z = \vec{v}_i \quad \text{at upward velocity} \quad (13)$$

$$\vec{P}_z = \vec{P}_i \quad \text{at upward pressure} \quad (14)$$

$$\vec{c}_z = \vec{c}_i \quad \text{at upward concentration} \quad (15)$$

At the outlet boundary condition, the pressure of blood flow is considered with no viscous stress, as shown in Eq. (16). This boundary condition specifies vanishing viscous stress along with a Dirichlet condition on the pressure and the convective flux of the concentration outlet boundary condition is defined in Eq. (17)

$$\eta(\nabla\vec{v} + (\nabla\vec{v})^T \cdot n = 0 \ , \ \vec{P} = \vec{P}_0 \ \text{at outlet pressure} \quad (16)$$

$$n \cdot (-D\nabla\vec{c}) = 0 \ \text{at outlet concentration} \quad (17)$$

where η is kinematics viscosity, P_0 is atmospheric pressure and T is matrix transpose.

The left and the right boundary conditions of the artery walls are applied at no slip, as shown in Eq. (18) This is the standard and default boundary condition for a stationary solid wall. The condition prescribed:

$$\vec{v} = 0 \quad \text{at solid wall} \quad (18)$$

For the temperature field boundary condition, the left and the right boundary conditions of the axially symmetric surface are applied at the insulation wall (Eq. (19)) which is kept at a constant temperature. The condition prescribed:

$$\frac{\partial T}{\partial n} = 0 \quad (19)$$

The inlet and outlet temperature boundary condition are shown in from Eqs. (20) and (21), respectively which defined as

$$T = T_i \quad (20)$$

and

$$-n \cdot (-k\nabla T + \rho c_p \vec{v}\nabla T) = 0 \quad (21)$$

where T, T_α and ∇T are temperature, ambient temperature and temperature gradient, respectively.

3.4 Calculation procedure

A fine mesh is specified in the sensitive areas and the vertical 2D axisymmetric model is discretized using a triangular element. This study provides a variable mesh method for solving the problem as shown in Fig. 6.

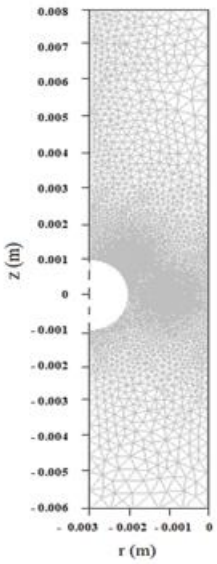

Fig. 6 The axially symmetric finite element meshes

The Lagrange quadratic is then used to approximate the electric field, the flow field, the concentration field, and the blood flows across each element for the prediction of the blood flow transport. This convergence test leads to the mesh with approximately 10,000 elements. With percentage error is lower than 0.1 and a dimensionless time step of 1 x 10^{-4} to ensure numerical stability and accuracy. The system of governing equations is solved with the unsymmetrical multi-frontal method. The accuracy of the simulation results is independent on the number of elements and therefore save computation memory and time. Higher numbers of elements are not tested due to lack of computational memory and performance.

4. Results and discussion

Blood flow transport with electrokinetic flow through the narrow semicircle shape within the vertical 2D asymmetrical model is systematically proposed. Numerical modeling combined with the electrostatics model, the flow and the concentration field model, and the temperature model. In this numerical study, the vertical 2D asymmetrical model is symmetrically investigated because many researchers numerically studied the horizontal 2D asymmetrical model. There are few studies on the vertical 2D asymmetrical model due to the complexity of the numerical model. The first part, the blood flow transport within the vertical 2D asymmetrical model has been compared to the electric field, the flow pattern, the pressure field, the vorticity, the temperature field, and the concentration field with and without the electrokinetic flow. After that, the blood flow is transported with the electrokinetic flow within the vertical 2D asymmetrical model in various electrical voltages and times. The last part shows the model validation in order to verify the accuracy of Finite Element Method (FEM) and experimental setup.

4.1 Comparison of blood flow transport without electrokinetic flow within the vertical 2D asymmetrical model

Without electrokinetic flow, the blood flow transport within the vertical 2D asymmetrical model is shown in Fig. 7. For all cases, the blood flow is moved upward through the vertical 2D asymmetrical model. In Fig. 7 (a), the electric field has not appeared because the electrical voltage is not included in the blood flow. Due to the initial condition is set up the initial velocity of the blood flow so the flow pattern is moved from the bottom to the top of the vertical 2D asymmetrical model and the blood flow avoided the semicircle shape, as shown in Fig. 7 (b). The flow pattern is the way in which blood moves through the vertical 2D asymmetrical model. The semicircle shape is set out of boundary condition and it appeared on the left of the vertical 2D asymmetrical model. In addition, the zero velocity fields (Stagnant zone or dead zone) have appeared at the left of the blood flow behind the vertical 2D asymmetrical model and it is avoided the narrow semicircle shape. For Fig. 7 (c), the pressure field of the left zone is lower than the right zone when it passes the semicircle zone. A pressure field is a two-component vector force field, which describes in a covariant way the dynamic pressure of individual particles and the pressure emerging in systems with a number of closely interacting particles. The vorticity field of the blood flow within the vertical 2D asymmetrical model is turbulence behind the semicircle zone, as shown in Fig. 7 (d). The vorticity is a pseudovector field that describes the local spinning motion of a continuum near some point. From Fig. 7 (e), the contour of temperature is more turbulent when it is near the semicircle zone. In addition, the concentration field of the blood flow is moved from the bottom to the top and it avoided the semicircle area as shown in Fig. 7 (f).

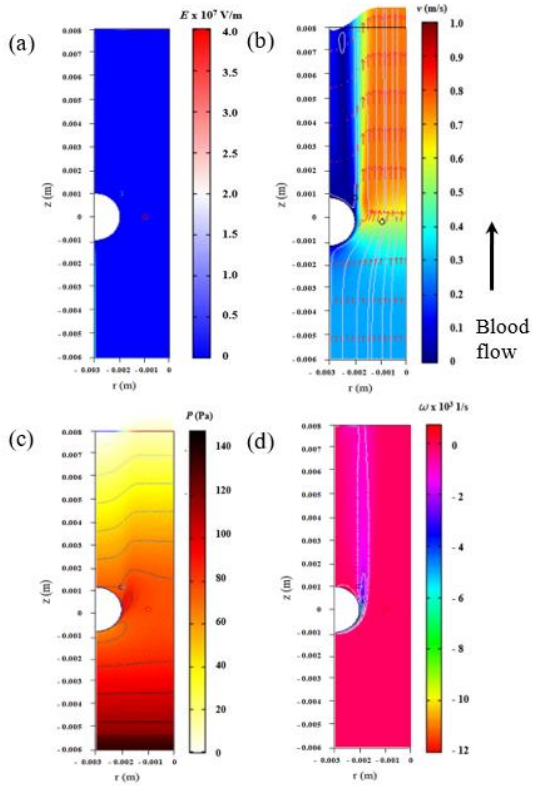

Fig. 7 Blood flow within the vertical 2D asymmetrical model in various values:)a(electric field)b(flow pattern)c(pressure field)d(vorticity (e) temperature field (f) concentration field without electrokinetic flow

In chemistry, the concentration is the abundance of a constituent divided by the total volume of a mixture. Furthermore, the flow

pattern, the pressure field, the temperature field, and the concentration field of the right side are more speed than the left side at the outlet axially symmetric surface and the upstream is more valuable than the downstream.

4.2 Comparison of blood flow transport with electrokinetic flow within the vertical 2D asymmetrical model

With electrokinetic flow, the electrical voltage is varied in order to consider the electric field, the flow pattern, the pressure field, the vorticity field, the temperature field, and the concentration field of the blood flow transport within the vertical 2D asymmetrical model. The electric field line in various electrical voltages is shown in Fig. 8. When electrical voltage is applied, the electric field moves outwardly from the tip of the electrode to the ground and it is concentrated at both the electrode and the ground area. The electric field line in the case of high electrical voltage (V_0 = 20 kV) (Fig. 8 (d)) is more concentrated than in the case of low electrical voltage (V_0 = 5 kV) (Fig. 8 (a)). It can be seen that the electric field is more concentrated when a higher electrical voltage is applied and the characteristic of the electric field is the same pattern in each case, as shown in (Fig. 8 (a - d)). These electric field lines can be used as representative of fluid motion driven by the electrophoretic force so it can change the flow visualization.

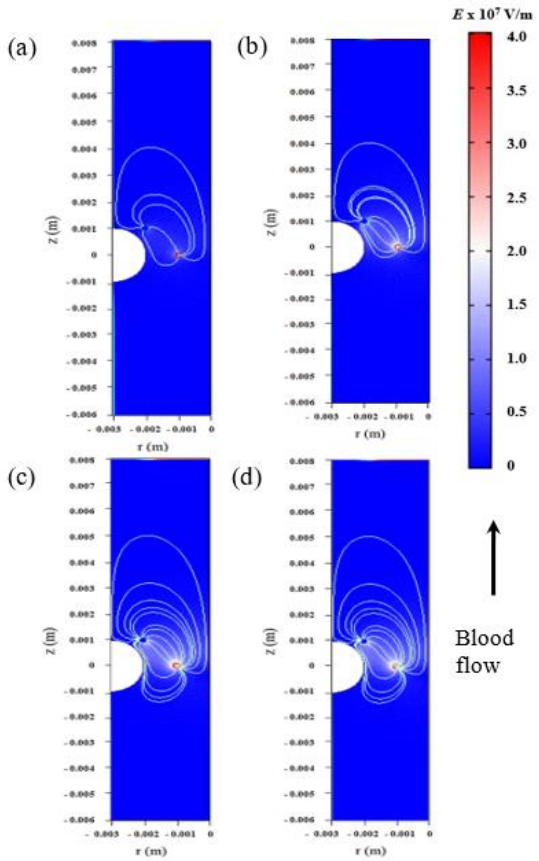

Fig. 8 Electric field within the vertical 2D asymmetrical model with electrokinetic flow in various electrical voltage (V_0)) a) V_0 = 5 kV (b) V_0 = 10 kV (c) V_0 = 15 kV (d) V_0 = 20 kV with electric field line

The flow pattern with a deformed shape, streamline, and arrow plot is compared in various electrical voltages, as shown in Fig. 9. The flow pattern is not the same pattern of the electric field but it is induced by the electric field. Within the vertical 2D asymmetrical model, the flow pattern is moved from the bottom to the top and the blood flow is avoided the semicircle shape, as shown in Fig. 9 (a - d). The stagnant zone appeared at the left of the blood flow behind the plaque deposits, and the blood flow slowly moved. The stagnant zone in the case of high electrical voltage (V_0 = 20 kV) (Fig. 9 (d)) is lower than in the case of low electrical voltage (V_0 = 5 kV) (Fig. 9 (a)). The high electrical voltage can reduce the stagnant zone within the vertical 2D asymmetrical model so the blood flow is increased at the destination.

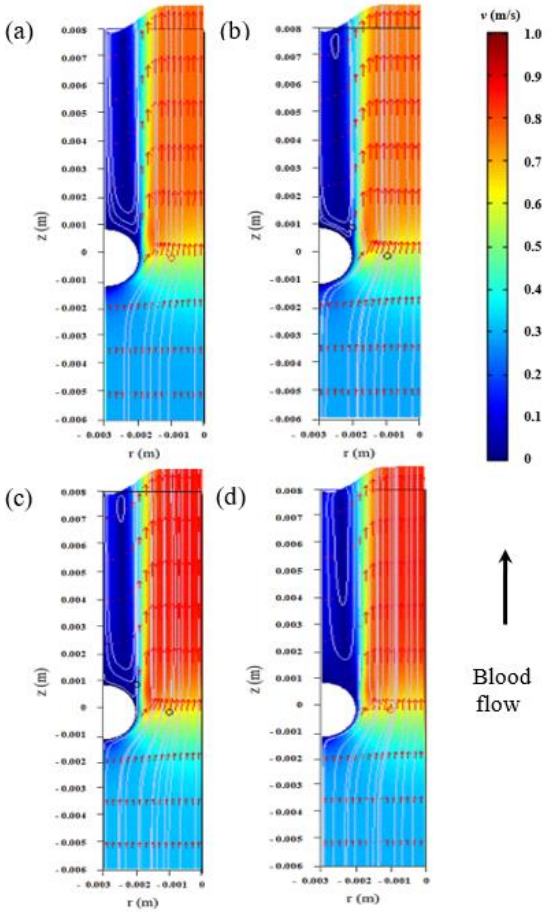

Fig. 9 Flow pattern of blood flow with electrokinetic flow within the vertical 2D asymmetrical model (a) V_0 = 5 kV (b) V_0 = 10 kV (c) V_0 = 15 kV (d) V_0 = 20 kV with deformed shape, streamline and arrow plot

The pressure field with a deformed shape and contour line is compared in various electrical voltages, as shown in Fig. 10. The pressure field within the vertical 2D asymmetrical model is influenced by the electric field. The pressure field is moved from the bottom to the top but the left of the pressure is lower than the right when it passes the semicircle zone, as shown in Fig. 10 (a - d). The pressure field in the case of low electrical voltage (V_0 = 5 kV) (Fig. 10 (a)) is lower than in the case of high electrical voltage (V_0 = 20 kV) (Fig. 10 (d)).

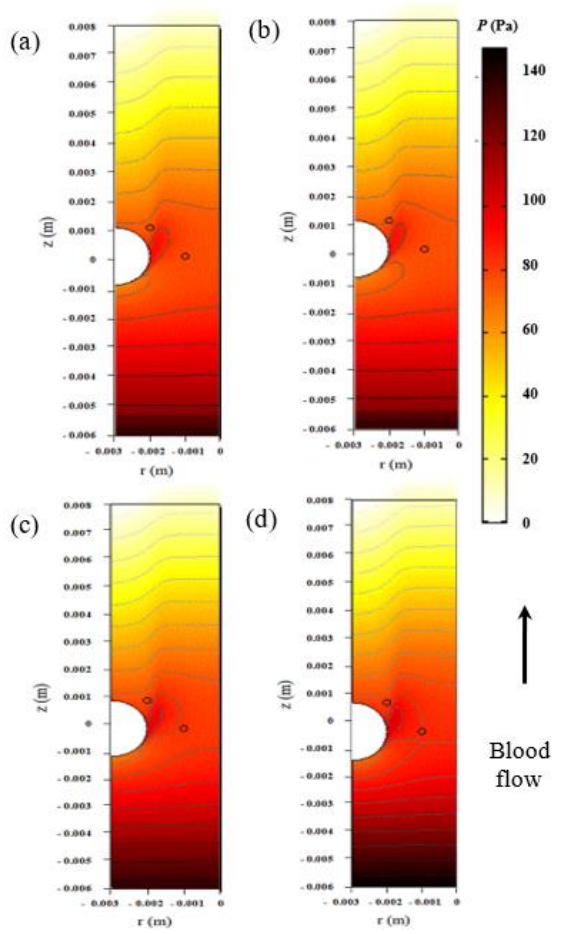

Fig. 10 Pressure field of blood flow with electrokinetic flow within the vertical 2D asymmetrical model (a) V_0 = 5 kV (b) V_0 = 10 kV (c) V_0 = 15 kV (d) V_0 = 20 kV with deformed shape and contour line

The vorticity field with a contour line is compared in various electrical voltages, as shown in Fig. 11. The vorticity field within the vertical 2D asymmetrical model is influenced by the electric field and it is turbulence behind the semicircle zone, as shown in Fig. 11 (a - d). The vorticity field in the case of low electrical voltage (V_0 = 5 kV) (Fig. 11 (a)) is more turbulent than in the case of high electrical voltage (V_0 = 20 kV) (Fig. 11 (d)) due to the vorticity field being more concentrated when the low electrical voltage.

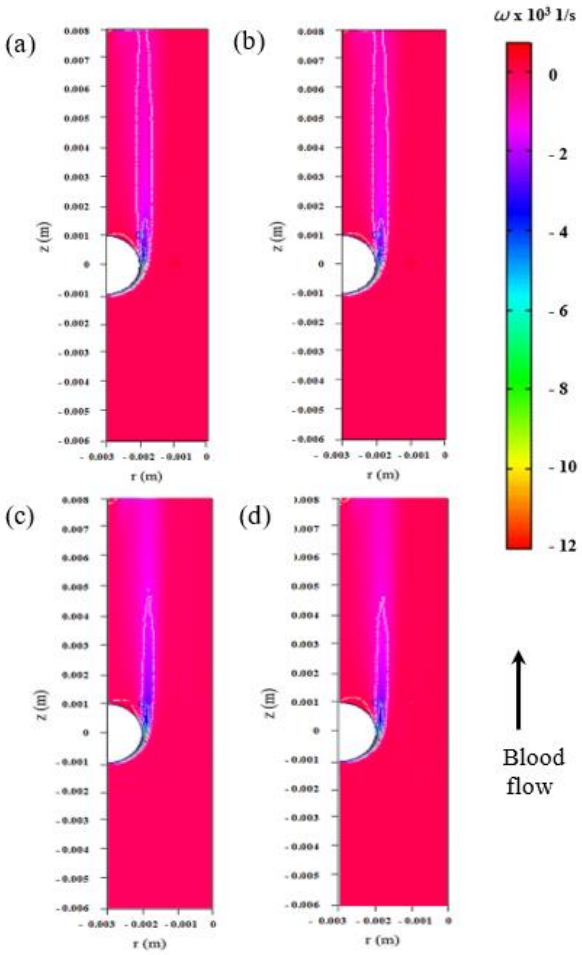

Fig. 11 Vorticity of blood flow with electrokinetic flow within the vertical 2D asymmetrical model (a) V_0 = 5 kV (b) V_0 = 10 kV (c) V_0 = 15 kV (d) V_0 = 20 kV with contour line

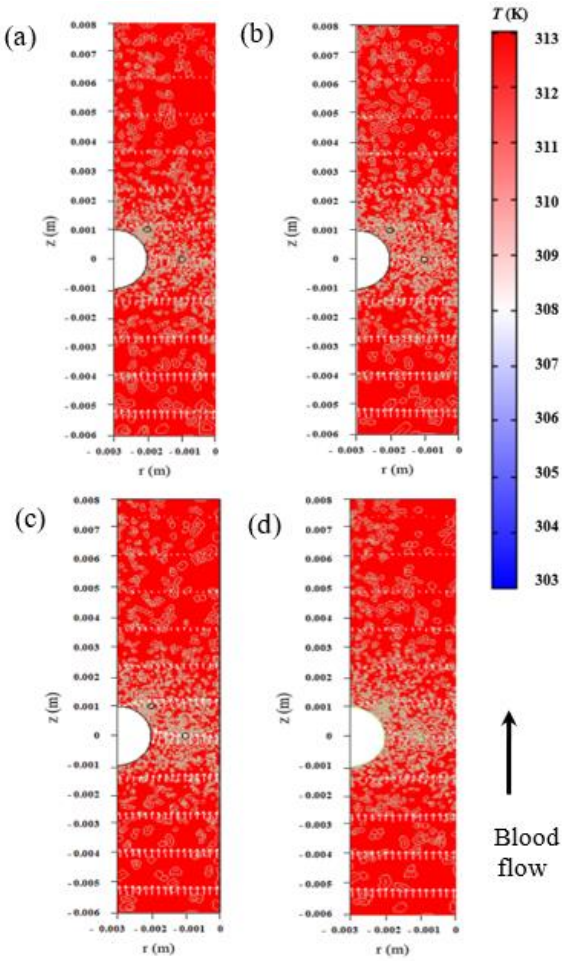

Fig. 12 Temperature field of blood flow with electrokinetic flow within the vertical 2D asymmetrical model (a) V_0 = 5 kV (b) V_0 = 10 kV (c) V_0 = 15 kV (d) V_0 = 20 kV with arrow plot and contour line

The temperature field with an arrow plot and contour line is compared in various electrical voltages, as shown in Fig. 12. The temperature within the vertical 2D asymmetrical model is still 310 K, and temperature is disturbed by the electrokinetic flow around the semicircle area, as shown in Fig. 12 (a - d). The temperature field in the case of high electrical voltage (V_0 = 20 kV) (Fig. 12 (d)) is more turbulent n in the case of low electrical voltage (V_0 = 5 kV) (Fig. 12 (a)).

The concentration field with a deformed shape and contour line is compared in various electrical voltages, as shown in Fig. 13. The concentration field within the vertical 2D asymmetrical model is influenced by the electric field. The concentration field is moved upward but the left of the concentration field is lower than the right when it passes the semicircle zone, as shown in Fig. 13 (a - d). The concentration field in the case of low electrical voltage (V_0 = 5 kV) (Fig. 13 (a)) is higher than in the case of high electrical voltage (V_0 = 20 kV) (Fig. 13 (d)).

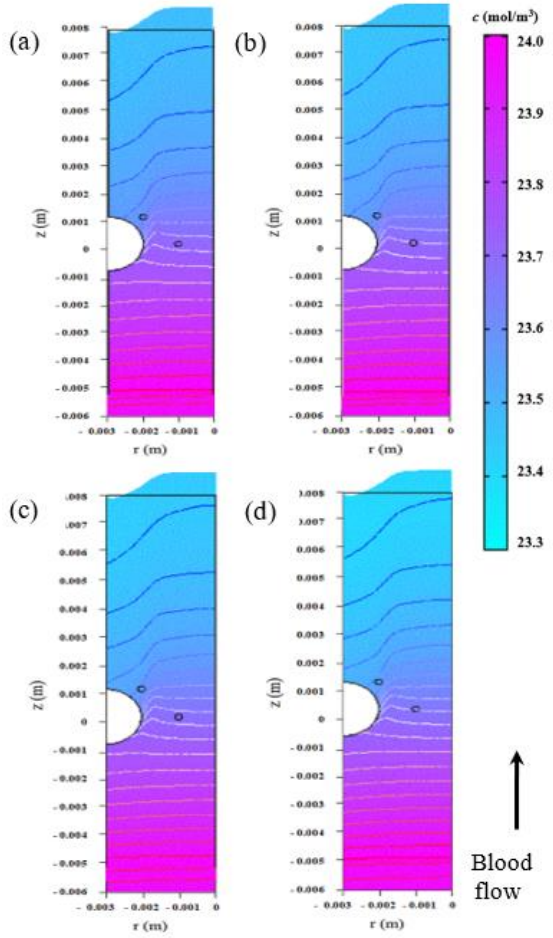

Fig. 13 Concentration field of blood flow with electrokinetic flow within the vertical 2D asymmetrical model (a) V_0 = 5 kV (b) V_0 = 10 kV (c) V_0 = 15 kV (d) V_0 = 20 kV with deformed shape and contour line

From the above data, the blood flow is moved upward through the vertical 2D asymmetrical model and it is avoided the narrow semicircle shape. The electric field is increased with the electrical voltage increasing. The flow pattern, the pressure field, the vorticity field, the temperature field, and the concentration field are not the same pattern as the electric field but they are induced by the electric field. In addition, the pressure field is the same pattern as the concentration field.

4.3 Analysis of blood flow transport with electrokinetic flow within the vertical 2D asymmetrical model

The electrokinetic flow within the vertical 2D asymmetrical model is analyzed at the center of the blood flow transport. The electrical voltage and time are varied in order to consider the electric value, the velocity, the pressure, the vorticity, the temperature, and the concentration of the blood flow transport. In various electrical voltages, the electric value, the velocity, the pressure, the vorticity, and the concentration are compared to the blood flow transport. Fig. 14 shows the development of the electrokinetic flow at the center of the narrow semicircle shape within the vertical 2D asymmetrical model. The time (t) is tested from 0 to 1 s by increments of 0.1 and the electrical voltage (V_0) is tested in 0, 8, and 16 kV. The electrical value does not depend on the time but it is increased with the electrical voltage increasing, as shown in Fig. 14 (a). For Fig. 14 (b), the velocity is zero for the first time (t = 0 s) and it is rapidly increased after the first time (t = 0.1 s). After that, the velocity is constant until the end of time (t = 1 s). For Fig. 14 (c), the low pressure is presented for the first time (t = 0 s) and it is little increased after the first time (t = 0.1 s). After that, the pressure is constant until the end of time (t = 1 s). The vorticity has a high value the first time (t = 0 s) and it is rapidly decreased after the first time (t = 0.1 s), as shown in Fig. 14 (d). After that, the vorticity is constant until the end of time (t = 1 s). At the first time (t = 0 s), the high electrical voltage (V_0 = 16 kV) can more disturb the vorticity than the low electrical voltage (V_0 = 8 kV), and the without electrical voltage (V_0 = 0 kV), but the vorticity is rapidly decreased after the first time (t = 0.1 s) until the end of time (t = 1 s). It can be seen that the electrokinetic flow can accelerate the blood flow to the outlet so the vorticity is decreased turbulent. The normal human body temperature (normothermia, euthermia) is the typical temperature range found in humans. The normal human body temperature range is typically stated as 97.7 – 99.5 °F (309.5 – 310.5 K). Body temperature is kept in the normal range by thermoregulation, in which adjustment of temperature is triggered by the central nervous system. Blood temperature is usually around 98.6 °F (310 K). From Fig. 14 (e), the electric field is not changing the temperature of blood so the property of blood is not changed. The concentration has a high value the first time (t = 0 s) and it is decreased after the first time (t = 0.1 s), as shown in Fig. 14 (f). After that, the concentration is constant until the end of time (t = 1 s). It can be seen that the electric

value, the velocity, and the pressure are increased with the electrical voltage increasing but the vorticity and the concentration are decreased with the electrical voltage increasing. After the first time (t = 0.1 s), the velocity is rapidly increased and the vorticity is rapidly decreased but the pressure is little increased and the concentration is decreased. This is because the electrokinetic flow technique is involved with the electro-fluid dynamics so the electric field can more disturb the flow pattern and the vorticity field than the pressure field, temperature field, and concentration field.

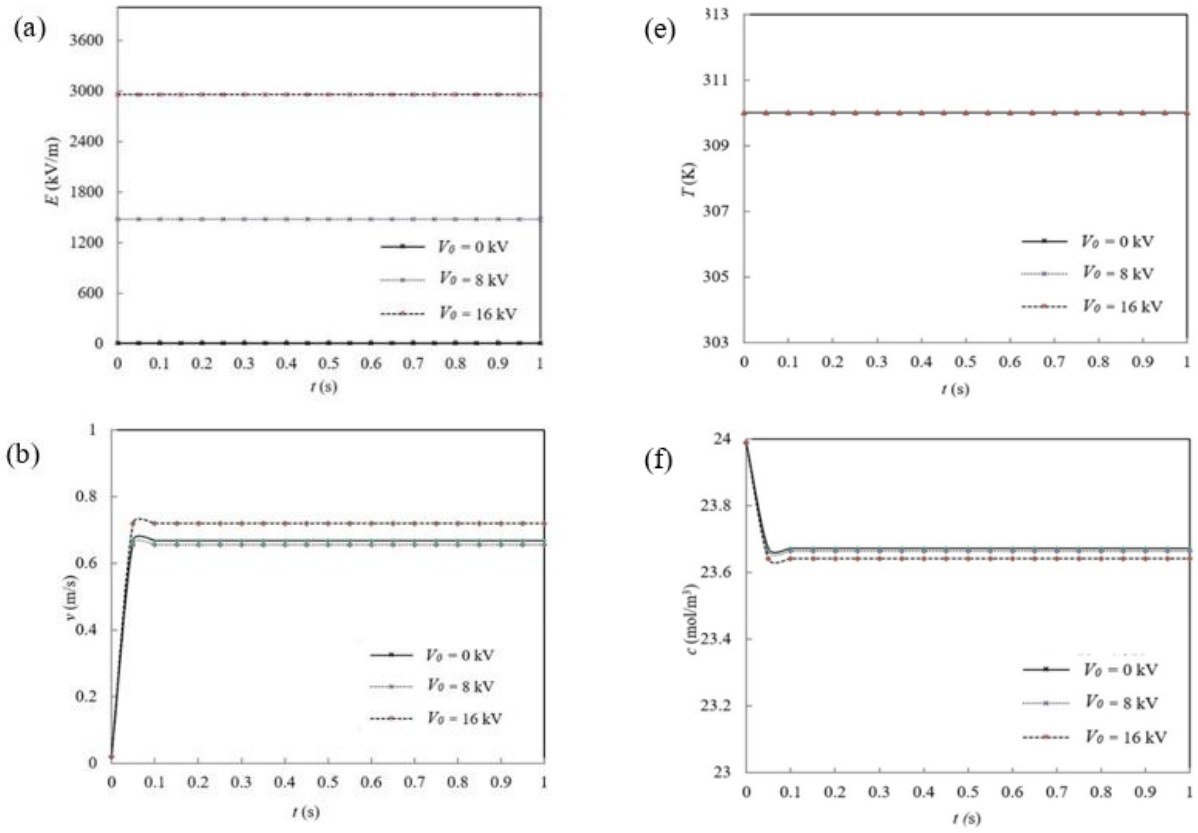

Fig. 14 Development of electrokinetic flow at the center of narrow semicircle shape within the vertical 2D asymmetrical model with various times when V_0 = 0, 8, and 16 kV (a) Electric value (b) Velocity (c) Pressure (d) Vorticity (e) Temperature (f) Concentration

For Fig. 15, the time (t) is fixed at 1 s and the electrical voltage (V_0) is varied from 0 to 20 kV by increments of 1. At the center of blood flow with the electrokinetic flow within the vertical 2D asymmetrical model, the electric field with the electrokinetic flow is increased with the

electrical voltage increasing but the temperature is gradually constant with the electrical voltage increasing. A comparison between the electric value and temperature is shown in Fig. 15 (a). A variable straight line for the electric field with the electrokinetic flow and electrical voltage ($E \propto V_0$). From Fig. 15 (b), the velocity and the pressure are increased with the electrical voltage increasing. The velocity and the pressure with the electrokinetic flow are proportional to the square of the electrical voltage ($v \propto P \propto V_0^2$). From Fig. 15 (c), the vorticity and the concentration are gradually decreased with the electrical voltage increasing. It can be seen that the velocity and the pressure graph are the same trends and the vorticity and the concentration graph are the same trends but the graph of the electrical field is different from other values.

For Fig. 16, the time (t) is fixed at 1 s and the electrical voltage (V_0) is varied from 0 to 20 kV by increments of 1. At the center of the narrow semicircle shape, the velocity ratio (the velocity under *EHD* per the velocity without *EHD*; v_{EHD}/v_{noEHD}) and the pressure ratio (the pressure under *EHD* per the pressure without *EHD*; P_{EHD}/P_{noEHD}) are increased with the electrical voltage increasing, as shown in Fig. 16 (a). The velocity ratio and the pressure ratio are proportional to the square of the electrical voltage ($v_{EHD}/ v_{noEHD} \propto P_{EHD}/P_{noEHD} \propto V_0^2$) and these results are related to the velocity and the pressure with the electrokinetic flow. From Fig. 16 (b), the vorticity ratio (the vorticity under *EHD* per the vorticity without *EHD*; $\omega_{EHD}/\omega_{noEHD}$) is decreased with the electrical voltage increasing but the concentration ratio (the concentration under *EHD* per the concentration without *EHD*; c_{EHD}/c_{noEHD}) is gradually constant with the electrical voltage increasing. The vorticity ratio is decreased proportionally to the square of the electrical voltage ($\omega_{EHD}/\omega_{noEHD} \propto 1/V_0^2$). It can be seen that the electrokinetic flow can increase the velocity ratio and the pressure ratio but it can decrease the vorticity ratio of the blood flow within the vertical 2D asymmetrical model. In addition, the electrokinetic flow hardly changed the concentration ratio and the temperature of the blood flow so the property of the blood does not change.

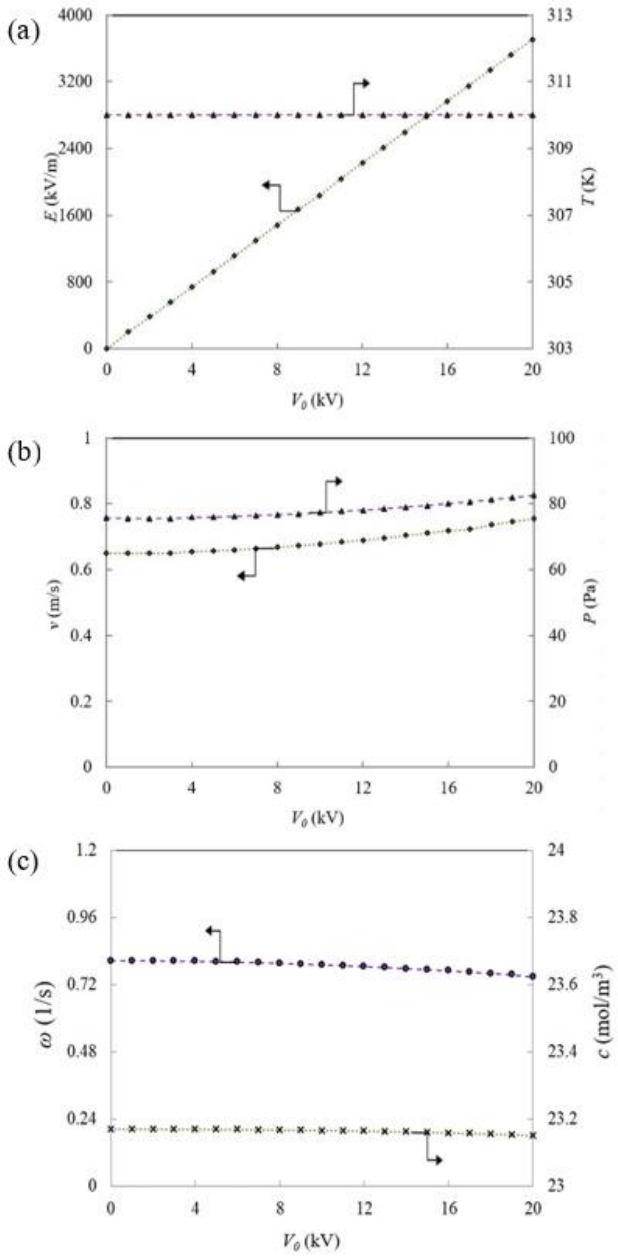

Fig. 15 Consider the center of the narrow semicircle shape within the vertical 2D asymmetrical model with t = 1 s and various electrical voltage (V_0) (a) Comparison between electric value and temperature (b) Comparison between velocity and pressure (c) Comparison between vorticity and concentration

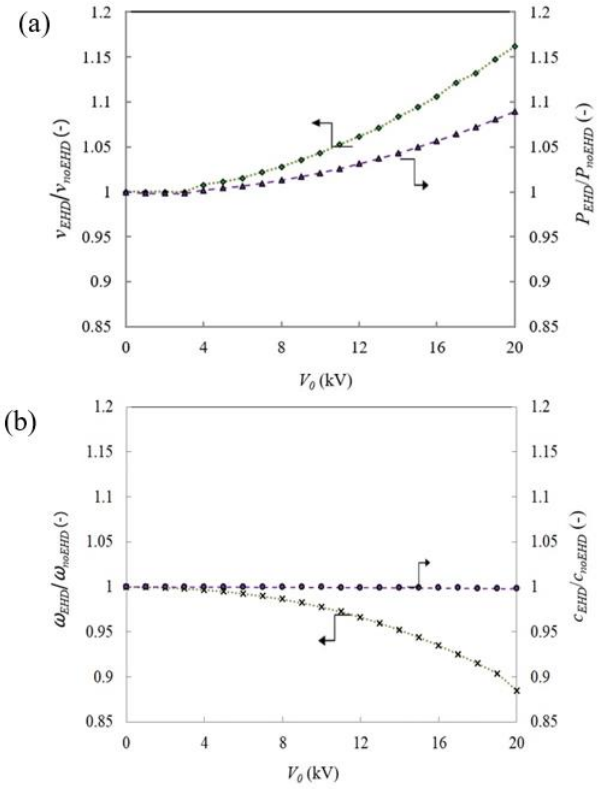

Fig. 16 Consider the center of the narrow semicircle shape with t = 1 s and various electrical voltage (V_0) (a) Comparison between velocity ratio and pressure ratio (b) Comparison between vorticity ratio and concentration ratio

Coronary heart disease involves the reduction of the blood flow to the heart muscle due to the plaque in the coronary heart. The plaque deposits stick at the artery wall so the pressure of the blood flow is low. But The pressure is the main factor for fluid-driven. This research shows the electric field, the flow field, the pressure field, the vorticity field, the concentration field, and the temperature field in the blood flow transport through the narrow semicircle shape with the electrokinetic flow model. The aim objective of this research is the increase the blood flow transport within the vertical 2D asymmetrical model. From above the result, the electric field is applied by the electrical voltage. The flow pattern, the pressure field, the vorticity field, the concentration field, and the temperature field of the blood flow transport are influenced by the electric field. In all cases, the blood flow transport is moved upward through the vertical 2D asymmetrical model. The pressure field is the same pattern as the concentration field but the electric field, the flow pattern, the vorticity field, and the temperature field have differences. The electric field can be used as representative of fluid motion driven by the electrophoretic force so the electrophoretic force can change the flow pattern, the pressure field, the vorticity field, the concentration field, and temperature the field. In addition, The velocity ratio is increased with the electrical voltage increasing and it is the same trend with the pressure ratio. The vorticity ratio is decreased with the electrical voltage increasing but the concentration ratio and the temperature are gradually constant with the electrical voltage increasing. Finally, with the influence of the electric field, the maximum velocity ratio and the maximum pressure ratio are increased by about 1.16 and 1.09 times, respectively. But the maximum vorticity ratio is decreased by about 1.14 times.

5. Model validation

In this topic, the validation is devided for 2 parts. The first part is compared between the experimental and numerical modeling, the blood flow transport through a narrow semicircle shape is analyzed from the diagram of corona arteries. For the second part, the numerical result from previous research is compared with the experimental result from present study.

5.1 Comperison between experimental and numerical modeling, the blood flow transport through a narrow semicircle shape is analyzed from the diagram of corona arteries

From experimental and numerical modeling, the blood flow transport through a narrow semicircle shape is analyzed from the diagram of corona arteries (Fig. 1 and 2). The electrokinetic flow techniques with and without the electrokinetic flow are clearly observed in order to predict the biomechanics therapy for the special design of the therapy of heart disease. The schematic diagram of the flow visualization using oil smoke incense technique is analyzed in Fig. 17. The inlet jet flow of smoke is created from an oil smoke generator with a blower and the oil smoke flowed upward within the wind tunnel. The controlled temperature is 25 ^{o}C and the inlet jet flow of smoke is supplied at 1 m/s. The wind tunnel is mostly made of acrylic plate and the experimental setup is an open system. For the

two-dimensional model for analysis, the dimension of the test section is 9.0 cm (high) x 6.0 m (wide). The two semicircles are stuck at the tunnel wall within the test section and they are obstacles to the smoke flow. The diameter of the semicircle is 4.0 cm and it is instead the plaque deposits. The high-voltage power supply (ACOPIAN model: NO30HP2M.-230) is used to create electrical voltage. The electrode and ground are made of copper wire and the electrode is fixed in front of the ground. The electrical high voltage (V_0) is fixed at 10 kV and two spotlights of 500 W are placed at the outlet of the test section in order to clearly investigated the flow visualization.

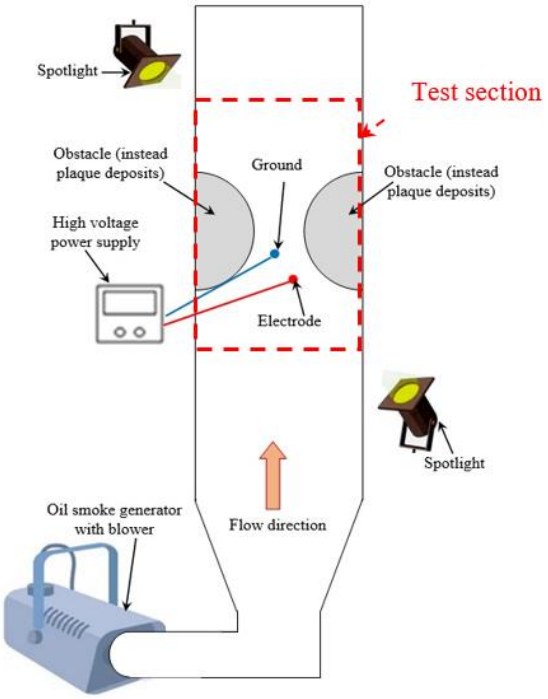

Fig. 17 The schematic diagram of the two-dimensional model for analysis

The flow visualization with and without the electrokinetic flow is experimentally and numerically studied from the schematic diagram in Fig. 17 and the boundary condition in Fig. 3, respectively. The experimental result of the flow field within the wind tunnel is shown in Fig. 18 and the numerical result of the flow field within the channel flow is shown in Fig. 19.

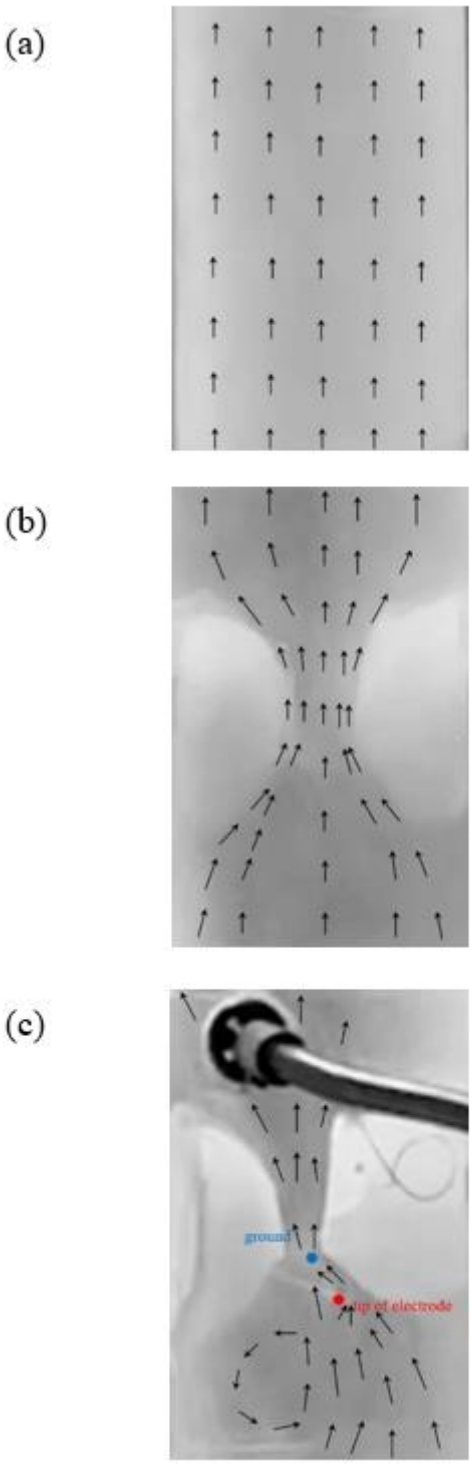

Fig. 18 Experimental result of the flow field within the wind tunnel (a) without electrokinetic flow (b) without electrokinetic flow and fluid flow through a narrow semicircle shape (c) with electrokinetic flow and fluid flow through a narrow semicircle shape

In the case of the normal artery and without electrokinetic flow, the diagram of the coronary artery and the boundary condition is investigated in Fig. 1 (a) and Fig. 3 (a), respectively. In fact, the coronary arteries supply blood to the heart muscle and it is transported upward through the coronary arteries. The fluid flow in the case of the experimental and numerical results are similar trends, as shown in Fig. 18 (a) and Fig. 19 (a). In the case without electrokinetic flow and fluid flow through a narrow semicircle shape, the semicircle is stuck instead of the plaque deposits and they are an obstacle to blood flow. The diagram of the coronary artery with blocked artery by plaque deposits and the boundary condition is investigated in Fig. 1 (b) and Fig. 3 (b), respectively. When plaque deposits substances build up in the walls of arteries. Over time, these plaques can narrow or completely block the arteries and cause problems throughout the body. From Fig. 18 (b), the oil smoke is moved from the bottom to the top of the wind tunnel and it avoided the semicircle shape. In addition, the flow field in the case of numerical results is shown in a similar trend to the experimental result, as shown in Fig. 19 (b). In the last case of the electrokinetic flow and fluid flow through a narrow semicircle shape, the diagram and the boundary condition are investigated in Fig. 2 and Fig. 3 (c), respectively. For the electrokinetic flow technique, the flow field is created by ions generated in the corona discharge near the sharp electrode that drift to the ground. The primary flow is generated from blower and the shear flow is then appeared due to difference of fluid velocity between charged airflow and uncharged airflow. As a result, the secondary flow is appeared. For Fig. 18 (c), the oil smoke is turbulent from the tip of the electrode and it is concentrated at both the electrode and the ground area. It can be seen that the stronger decondary flow due to the effect of electric field distribution is clearly shown around the ground where the secondary flow displays in counterclockwise direction when oil smoke is supplied in left direction. In the case of a numerical investigation, it can observe the streamline of the flow field, as shown in Fig. 19 (c). The electrokinetic flow technique can increase the disturbance of fluid and the secondary flow can increase the turbulence flow. It can be seen that EHD or electrokinetic flow technique can increase the velocity and the turbulence of the fluid flow [3]. Furthermore, the velocity in the case of the electrokinetic flow technique (Fig. 18 (c) and Fig. 19 (c)) can more increase than in the case of without the electrokinetic flow technique (Fig. 18 (b) and Fig. 19 (b)).

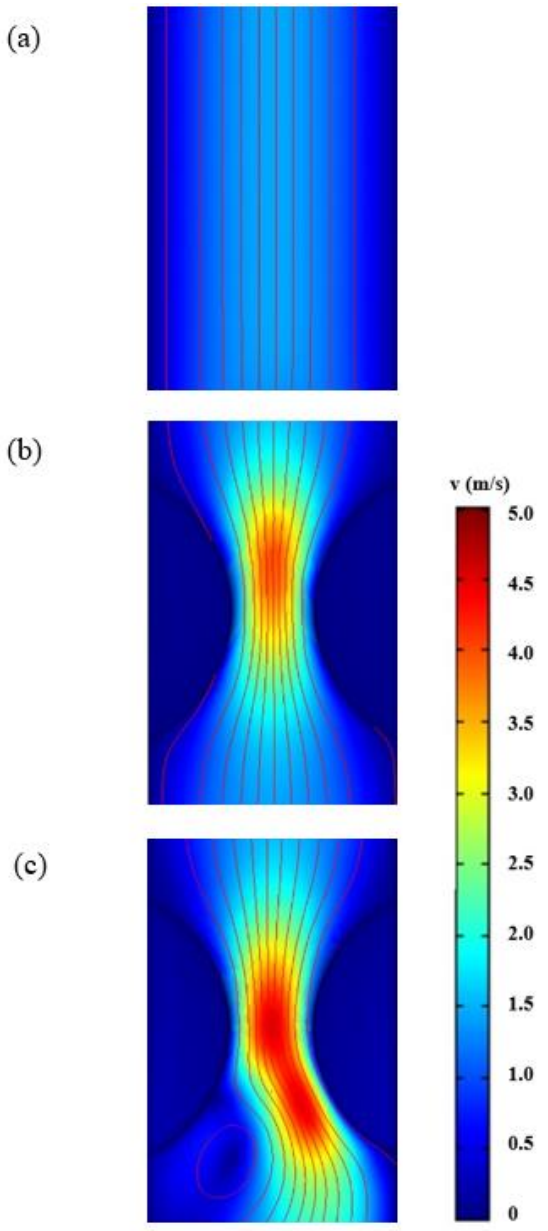

Fig. 19 Numerical result of the flow field within channel flow (a) without electrokinetic flow (b) without electrokinetic flow and fluid flow through a narrow semicircle shape (c) with electrokinetic flow and fluid flow through a narrow semicircle shape

5.2 Comperison between the numerical result from previous research and the experimental result from present study

To verify the accuracy of Finite Element Method (FEM), the present study was validated against the resulting data of previous studies. From numerical result, the velocity field from the previous study by Saneewong Na Ayuttaya [29] was studied with various angle of inclined flat plate and electrical voltage. The present result is studied from experimental result. Schematic diagrams of jet airflow impact inclined flat plate for the two-dimensional model for analysis are shown in Fig. 20. Dimension of tunnel are 1.5 m (long) x 0.3 m (high) x 0.3 m (wide). The jet airflow is supplied from a blower at 1 m/s (u_i = 1 m/s) and the air is moved in the left to the right direction. The outlet diameter of a nozzle jet is 1 cm. The high voltage power supply (ACOPIAN model: NO30HP2M.-230) is used to create an electrical voltage and the electrical high voltage (V_0) is varied from 0 to 30 kV. The dimension of the inclined flat plate is 15x15 cm^2 and the angle of the inclined flat plate (θ) is varied in the range of 15, 45 and 75°. The gap between the electrode plate and the ground flat plate are fixed at 4 cm. The impact velocity (u) under electrokinetic flow is measured by a flow meter.

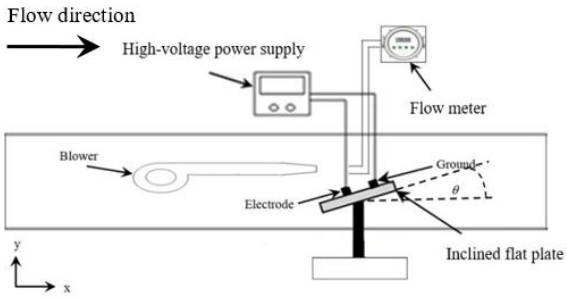

Fig. 20. Two-dimensional model

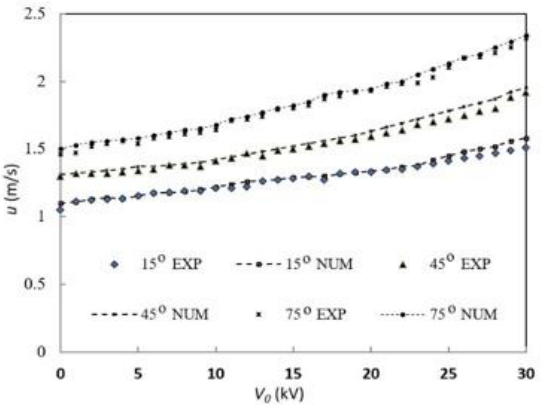

Fig. 21 Comparison of impact velocity between experimental and numerical result in various the inclined flat plate and electrical voltage

Comparison of impact velocity between experimental and numerical result is shown in Fig. 21. The position of the impact velocity is attack at the middle of the inclined flat plate and between of electrode and ground area. It can be seen that the impact velocity is increased with increasing the electrical voltage and the angle of the inclined flat plate. In addition, a similar trend of the graph has appeared for experimental and numerical results so simulation results had good agreement with experiment results.

From the above results, the fluid flow in all cases of the experimental and numerical results are similar trends. It can be seen that the idea behind this research can be used as implementation guidance for special design in the future for the biomechanical of heart disease therapy with the electrokinetic flow technique.

6. Conclusions

The numercal result is carried out to study the influences the blood flow transport with the electrokinetic flow technique through a narrow semicircle shape in the 2D asymmetrical model. The following are the conclusions of this research.

The electric field is more concentrated when a higher electrical voltage is applied. The flow pattern, the pressure field, the vorticity field, the concentration field, and the temperature field are not the same pattern as the electric field but it is induced by the electric field. The electrical voltage does not depend on the time but it is increased with the electrical voltage increasing. The electric value, the velocity, and the pressure are

increased with the electrical voltage increasing but the vorticity and the concentration are decreased with the electrical voltage increasing. The electric field can increase the velocity ratio and the pressure ratio but it can decrease the vorticity ratio of the blood flow in the coronary heart. The concentration ratio and the temperature is gradually constant with the electrical voltage increasing so the electrokinetic flow is not influenced by the property of the blood flow.

Acknowledgments

This research was conducted at the Chulachomklao Royal Military Academy Fund and Department of Mechanical Engineering, Faculty of Engineering, Rajamangala University of Technology Rattanakosin for their support of this study.

References

[1] C. Yang, Y. Kang, X. Huang, Electrokinetic Flow in Porous Media. Encyclopedia of Microfluidics and Nanofluids 92(2007) 506 – 516.

[2] S. Rashidi, H. Bafekr, M.S. Valipour, J.A. Esfahani, A review on the application, simulation, and experiment of the electrokinetic mixers. Chemical Engineering and Processing - Process Intensification 126 (2018) 108 - 122.

[3] S. Saneewong Na Ayuttaya, Heat transfer enhancement on saturated porous samples using electrostatic precipitator process in k-ε turbulent model. International Journal of Thermofluid Science and Technology 9(4) (2022) 090403.

[4] M.M. Bhatti, F. Ishtiaq, R. Ellahi, S.M. Sait, Novel Aspects of Cilia-Driven Flow of Viscoelastic Fluid through a Non-Darcy Medium under the Influence of an Induced Magnetic Field and Heat Transfer. Mathematics 11(10) (2023) 2284.

[5] M. Wang, J. Wang, S. Chen, N. Pan, Electrokinetic pumping effects of charged porous media in microchannels using the lattice Poisson–Boltzmann method. Journal of Colloid and Interface Science 304)2006(246 – 253.

[6] Y. Kang, S.C. Tan, C. Yang, X. Huang, Electrokinetic pumping using packed microcapillary. Sensors and Actuators A 133133 (2007) 375 – 382.

[7] C.L.A. Berli, Output pressure and efficiency of electrokinetic pumping of non- Newtonian fluids. Microfluid Nanofluid 8)2010(197 – 207.

[8] A. Jaworek, Electrospray droplet sources for thin film deposition. Journal of Materials Science 42)2007(266 – 297.

[9] M. Oss, A. Kruve, K. Herodes, I. Leito, Electrospray ionization efficiency scale of organic compounds. Analytical Chemistry 82(7) (2010) 2865 – 2872.

[10] S.M.E. Haque, M.G. Rasul, A.V. Deev, M.M.K. Khan, N. Subaschandar, Flow simulation in an electrostatic precipitator of a thermal power plant. Applied Thermal Engineering 29 (2009) 2037 – 2042.

[11] H. Nouri, N. Zouzou, E. Moreau, L. Dascalescu, Y. Zebboudj, Effect of relative humidity on currente voltage characteristics of an electrostatic precipitator. Journal of Electrostatics 70)2012(20 - 24.

[12] M.C. Zaghdoudi, M. Lallemand, Pool boiling heat transfer enhancement by means of high DC electric field. The Arabian Journal for Science and Engineering 30(2B) (2005) 189 – 212.

[13] A. Shahriari, P. Birbarah, J. Oh, N. Miljkovic, V. Bahadur, Electric field–based control and enhancement of boiling and condensation. Nanoscale and Microscale Thermophysical Engineering 21(2) (2017) 102 – 121.

[14] G. Wang, Z. Zhang, R. Wang, Z. Zhu, A review on heat transfer of nanofluids by applied electric field or magnetic field. Nanomaterials 10 (2020) 1 – 24.

[15] J.K. Singh, S. Vishwanath, Hall and induced magnetic field effects on convective flow of viscoelastic fluid within an inclined channel with periodic surface conditions. International Journal of Thermofluid Science and Technology 7(4))2020(070402.

[16] M.Z. Bazant, T.M. Squires, Induced-charge electrokinetic phenomena. Current Opinion in Colloid & Interface Science 15)2010(203 – 213.

[17] S.R.R. Reddy, H.T. Basha, P. Duraisamy, Entropy generation for peristaltic flow of gold-blood nanofluid driven by electrokinetic force in a microchannel. The European Physical Journal Special Topics 231 (2022) 2409 - 2423.

[18] M.M. Bhatti, S.M. Sait, R. Ellahi, Magnetic nanoparticles for drug delivery through tapered stenosed artery with blood based non-newtonian fluid. Phamaceuticals 15(11) (2022) 1352.

[19] T.J. Pianta, P.S. Baldwin, E.A. Silverstein, A biomechanical analysis of treatment options for enchondromas of the hand. Hand 8 (2013) 86 - 91.

[20] C.J. Roberts, W.J. Dupps, Biomechanics of corneal ectasia and biomechanical treatments. Journal of Cataract & Refractive Surgery 40(6) (2014) 991 - 998.

[21] R.J. Midura, M.O. Ibiwoye, K.A. Powell, Y. Sakai, T. Doehring, M.D. Grabiner, T.E. Patterson, M.

Zborowski, A. Wolfman, Pulsed electromagnetic field treatments enhance the healing of fibular osteotomie. Journal of Orthopaedic Research 23 (2005) 1035 - 1046.

[22] N.I. Lebovka, M. Shynkaryk, E. Vorobiev, Moderate electric Field treatment of sugarbeet tissues. Biosystems Engineering 96)1( )2007(47 – 56.

[23] P.C. Miranda, A. Mekonnen, R. Salvador, P.J. Basser, Predicting the electric field distribution in the brain for the treatment of glioblastoma. Physics in Medicine & Biology 59(15) (2014) 4137 - 4147.

[24] M. Venkateswarlu, P. Bhaskar, Entropy Generation and Bejan Number Analysis of MHD Casson Fluid Flow in a Micro-Channel with Navier Slip and Convective Boundary Conditions. International Journal of Thermofluid Science and Technology 7(4) (2020) 070403.

[25] M.M. Bhatti, A. Zeeshan, F. Bashir, S.M. Sait, R. Ellahi, Sinusoidal motion of small particles through a Darcy-Brinkman-Forchheimer microchannel filled with non-Newtonian fluid under electro-osmotic forces. Journal of Taibah University for Science 15(1) (2021) 514 – 529**.**

[26] R. Dadsetani, G.A. Sheikhzade, M. Goodarzi, A. Zeeshan, R. Ellabi, M.R. Safaei, Thermal and mechanical design of tangential hybrid microchannel and high-conductivity inserts for cooling of disk-shaped electronic components. Journal of Thermal Analysis and Colorimetry 143 (2021) 2125 – 2133.

[27] A. Zeeshan, F. Bashir. Alzahrani, Electro-osmosis-modulated biologically inspired flow of solid–liquid suspension in a channel with complex progressive wave: application of targeted drugging. Canadian Journal of Physics 100(3) (2022) 3 – 26.

[28] M. J. Uddin 1, A. K. M. Fazlul Hoque, M. M. Rahman, K. Vajravelu, Numerical simulation of convective heat transport within the nanofluid filled vertical tube of plain and uneven side walls. International Journal of Thermofluid Science and Technology 6(1) (2019) 19060101.

[29] S. Saneewong Na Ayuttaya, Numerical Analysis of Jet Airflow Impact Inclined Flat Plate under Electrohydrodynamics Force in a Porous Medium. International Journal of Numerical Methods for Heat and Fluid Flow 31(7) (2021) 2373 - 2404.

[30] D.J. Griffiths (1999). Introduction to electro-hydrodynamics. Prentice Hall International, Inc. New Jersey, 54.

[31] P. Montienthong, P. Rattanadecho, W. Klinbun, Effect of electromagnetic field on distribution of temperature, velocity and concentration during saturated flow in porous media based on local thermal non-equilibrium models (Influent of input power and input velocity). International Journal of Heat and Mass Transfer 106 (2017) 720 - 730.

[32] T.J. Arthur, Biomechanics and exercise physiology: Quantitative modeling, Taylor&Francis (2007) 29.

[33] T. Wessapan, S. Srisawatdhisukul, P. Rattanadecho, The effects of dielectric shield on specific absorption rate and heat transfer in the human body exposed to leakage microwave energy. International Communications in Heat and Mass Transfer 38(2) (2011) 255 – 262.